Doublet Strip Method for Oscillating Swept Tapered Wings in Incompressible Flow

A. Ichikawa*
Civil Aviation College, Miyazaki, Japan

An improved numerical method is developed for calculating the load distributions on oscillating swept tapered wings in incompressible flow. The integration domain is transformed into a rectangular domain, and the domain is divided into many chordwise strips. In the strip containing the control point, the proposed method properly accounts for Cauchy and logarithmic singularities. The solutions generally compared well with other lifting-surface theories, but with much smaller computational times.

Nomenclature

$\mathcal{R}$ = aspect ratio
A,B = see Eq. (12) or (52)
$\boldsymbol{B}$ = $\boldsymbol{K}/e^{ikx_0}$
b = wing span
$c(y)$ = wing semichord
c_0 = wing root semichord
c_R = wing root chord, $=2c_0$
c_τ = wing-tip chord
C_l = sectional lift coefficient
C_L = wing lift coefficient
C_p = lifting pressure coefficient, $=(p_- - p_+)/(\rho U^2/2)$
D^{ij}_{kl} = influence coefficient of RS, see Eqs. (10) and (54)
$\boldsymbol{K}$ = kernel function, see Eq. (3)
K^i_k = influence coefficient of SS, see Eq. (50)
k = reduced frequency, $=\omega c_0/U$
$m_{\rm LE}$ = $\tan\Lambda_{\rm LE}$
m_M = $\tan\Lambda_M$
$m_{\rm TE}$ = $\tan\Lambda_{\rm TE}$
Δ_m = $\tan\Lambda_{\rm TE}-\tan\Lambda_M$
NC = number of chordwise loading points
NS = number of spanwise loading points (semispan)
RS = regular strip (strip without control point)
SS = singular strip (strip with control point)
s = tip inset, see Eq. (8)
U = freestream velocity
w = downwash velocity, positive upward
w_L,w_R = downwash velocity induced by left and right wing panels, respectively
x,y = Cartesian coordinates, see Fig. 1
$x_M(y)$ = chordwise coordinate of mean chord line
x_0 = $x-x_1$
y_0 = $y-y_1$
ξ = nondimensional chordwise variable
θ = $\cos^{-1}(-\xi)$
λ = wing taper ratio, $=c_\tau/c_R$
$\Lambda_{\rm LE}$ = leading-edge sweep, deg
Λ_M = mean chord line sweep, deg
$\Lambda_{\rm TE}$ = trailing-edge sweep, deg
ρ = air density

Subscripts and Superscripts

i,j = chordwise and spanwise control points, respectively
k,l = chordwise and spanwise loading points, respectively
LE,TE = leading and trailing edges, respectively, of wing
$(^-)$ = complex amplitude or coordinate on left wing panel

Received July 2, 1984; revision received June 6, 1985. Copyright © American Institute of Aeronautics and Astronautics, Inc., 1985. All rights reserved.
*Associate Professor. Member AIAA.

Introduction

AERODYNAMIC characteristics of oscillating wings at subsonic speeds are generally calculated by doublet-lattice or lifting-surface methods. Doublet-lattice methods[1] are simpler and easier to apply to complex configurations than lifting-surface methods, but they require a relatively large number of unknowns ("boxes") for convergence.

To improve the convergence, the author has proposed an improved numerical method (doublet strip method[2]) for rectangular wings in incompressible flow. A key point of the method is to use an expansion series of the kernel[3] together with proper treatment of the chordwise logarithmic singularity.[4] Unlike conventional doublet-lattice methods, the proposed method uses many chordwise strips, and spanwise integration is performed first to avoid Mangler's principal values.

The purpose of the present paper is to extend the idea of the doublet strip method to involve swept tapered wings. The integration domain is transformed into a rectangular domain in order to apply a technique that has been developed previously in Ref. 2. The solutions generally compared well with other lifting-surface theories, but with much shorter computational times.

Doublet Strip Method

The coordinate system is illustrated in Fig. 1, where trapezoidal geometry is defined by

$$\lambda=c_\tau/c_R, \qquad c_R=2b/\mathcal{R}(1+\lambda)$$

$$m_M=\tan\Lambda_M$$

$$\Delta m=\tan\Lambda_{\rm TE}-\tan\Lambda_m=2(\lambda-1)/\mathcal{R}(\lambda+1) \tag{1}$$

The downwash equation in incompressible flow is

$$\frac{\bar{w}(x,y)}{U})=\frac{1}{8\pi}\cdot\int_{-b/2}^{b/2}\int_{x_{\rm LE}}^{x_{\rm TE}}\boldsymbol{K}(x_0,y_0;k)\bar{C}_p(x_1,y_1)\,dx_1\,dy_1 \tag{2}$$

$$\boldsymbol{K}(x_0,y_0;k)=e^{-ikx_0}\int_{-\infty}^{x_0}e^{ik\nu}\Big/(\nu^2+y_0^2)^{3/2}\,d\nu \tag{3}$$

A swept tapered domain can be transformed into a rectangular domain by introducing a new variable ξ, where

$$\xi(x, y) = \{x - x_M(y)\}/c(y) \quad -1 \leqq \xi \leqq 1 \tag{4}$$

is the nondimensional chordwise variable.

Since the forms of $x_M(y)$ and $c(y)$ on the left wing panel are different from those on the right wing panel, it is convenient to treat each wing panel separately. The total downwash at (ξ, y) on the swept wing is composed of the contribution from both wing panels and is defined by

$$\frac{\bar{w}(\xi,y)}{U} = \frac{1}{8\pi} \cdot \int_0^{b/2} \int_{-1}^{1} \boldsymbol{K}(x_0, y_0; k) \bar{C}_p(\xi_1, y_1) c(y_1) \mathrm{d}\xi_1 \mathrm{d}y_1 + \frac{1}{8\pi} \cdot \int_{-b/2}^{0} \int_{-1}^{1} \boldsymbol{K}(x_0, \bar{y}_0; k) \bar{C}_p(\xi_1, \bar{y}_1) c(\bar{y}_1) \mathrm{d}\xi_1 \mathrm{d}\bar{y}_1 \tag{5}$$

where

$$c(y_1) = y_1 \Delta m + c_0, \quad c(\bar{y}_1) = -\bar{y}_1 \Delta m + c_0 \tag{6}$$

Note that y_1 and $\bar{y}_1$ are the spanwise integration points on the right and left wing panels, respectively. Due to symmetry, control points are needed on the right wing panel only.

Downwash Contribution from the Right Wing Panel

The wing panel is divided into many chordwise strips by using uniform spacing with inset.[5] The strip containing the control point is named the singular strip (SS) and the other strips are named regular strips (RS). It is assumed that the continuous pressure distribution over the wing is replaced with the one that is constant in the spanwise direction on each strip. Then, the first integration of Eq. (5) can be written as

$$\left(\frac{\bar{w}_R}{U}\right)_{ij} = \frac{1}{8\pi} \cdot \sum_{l=1}^{NS}{}' \int_{d_l}^{d_{l+1}} \int_{-1}^{1} \boldsymbol{K}(x_0, y_0; k) \bar{C}_p(\xi_1, y_1) c(y_1) \mathrm{d}\xi_1 \mathrm{d}y_1 + \frac{1}{8\pi} \cdot \int_{y_i - e_1}^{y_i + e_2} \int_{-1}^{1} \boldsymbol{K}(x_0, y_0; k) \bar{C}_p(\xi_1, y_j) c(y_j) \mathrm{d}\xi_1 \mathrm{d}y_1 \tag{7}$$

where Σ' implies the exception of the singular strip, and

$$\begin{aligned} d_l &= b(1-s)/2 \cdot (l-1)/NS, \qquad l = 1,2,\ldots,NS+1 \\ y_{l(j)} &= b(1-s)/2 \cdot (2l(j)-1)/2NS, \qquad l,j = 1,2,\ldots,NS \\ s &= 1/4NS \end{aligned} \tag{8}$$

Regular Strip

Since the kernel function in the regular strip contains no singularity; the treatment of the integral is straightforward. Using the Gauss formula, the first integral of Eq. (7) is discretized to be

$$[\mathrm{RS}] = \frac{1}{4(2NC+1)} \cdot \sum_{l=1}^{NS}{}' \sum_{k=1}^{NC} D_{kl}^{ij} \bar{C}_{pkl} c(y_l) \sin\theta_k \tag{9}$$

$$D_{kl}^{ij} = \int_{d_l}^{d_{l+1}} \boldsymbol{K}(x_0, y_0; k) \mathrm{d}y_1 \tag{10}$$

where the positions of the control points and loading points are

$$\begin{aligned} \xi_i &= -\cos\theta_i, \quad \theta_i = 2i\pi/(2NC+1), \qquad i = 1,2,\ldots,NC \\ \xi_k &= -\cos\theta_k, \quad \theta_k = (2k-1)\pi/(2NC+1), \qquad k = 1,2,\ldots,NC \end{aligned} \tag{11}$$

respectively.

The spanwise integration of Eq. (10) is performed by the same method as in the Ref. 1 which uses a parabolic approximation. It must be noted that x_0 in Eq. (10) becomes

$$x_0 = Ay_0 + B, \quad A = m_M + \Delta m\xi, \quad B = (\Delta m y + c_0)(\xi - \xi_1) \tag{12}$$

by transforming the independent variable from x,y to ξ,y.

Singular Strip

Since the kernel function in the singular strip has several singularities, careful treatment is necessary. Using $\boldsymbol{K}(x_0,y_0;k) = e^{-ikx_0}\boldsymbol{B}(k, |y_0|, x_0) = e^{-ik(Ay_0+B)}\boldsymbol{B}(k, |y_0|, x_0)$, the singular strip term of Eq. (7) becomes

$$[\mathrm{SS}] = \frac{1}{8\pi} \cdot \int_{-e_2}^{e_1} \boldsymbol{B}(k, |y_0|, x_0) e^{-ikAy_0} \mathrm{d}y_0 \times \int_{-1}^{l} e^{-ikB} \bar{C}_p(\xi_1, y_j) c(y_j) \mathrm{d}\xi_1 \tag{13}$$

and the y_0-integration portion of the above equation is

$$I = I_1 + I_2 \tag{14}$$

$$I_1 = \int_{-e_2}^{e_1} \boldsymbol{B}(k, |y_0|, x_0) \mathrm{d}y_0 \tag{15}$$

$$I_2 = \int_{-e_2}^{e_1} \boldsymbol{B}(e^{-ikAy_0} - 1) \mathrm{d}y_0 \tag{16}$$

I_1 and I_2 are now evaluated.

A. I_1: Using an expansion series of the kernel,[3] I_1 becomes

$$I_1 = \hat{B}_R + i\hat{B}_I \tag{17}$$

$$\hat{B}_R = \hat{U}_0 - \hat{U}_2 + \int_{-e_2}^{e_1} \sum_{n=2}^{\infty} (-1)^n U_{2n} \mathrm{d}y_0 - \frac{k^2}{2} \times \sum_{n=0}^{\infty} \frac{1}{(n+1)(n!)^2} \left\{ \sum_{m=1}^{n} \frac{1}{m} + \frac{1}{2(n+1)} - \gamma - \ell n\left(\frac{k}{2}\right) \right\} \times \left(\frac{k}{2}\right)^{2n} \frac{e_1^{2n+1} + e_2^{2n+1}}{2n+1} \tag{18}$$

$$\hat{B}_I = \hat{U}_1 + \hat{U}_3 + \int_{-e_2}^{e_1} \sum_{n=2}^{\infty} (-1)^n U_{2n+1} \mathrm{d}y_0 + \frac{\pi k^2}{4} \times \sum_{n=0}^{\infty} \frac{1}{(n+1)(n!)^2} \times \left(\frac{k}{2}\right)^{2n} \frac{e_1^{2n+1} + e_2^{2n+1}}{2n+1} \tag{19}$$

$\hat{U}_0 \sim \hat{U}_3$ are given as

$$\hat{U}_0 = -[1/e_1 \cdot (1 + R_1/B) + 1/e_2 \cdot (1 + R_2/B)] \tag{20}$$

$$\hat{U}_1 = -k\tilde{I}_F + 2k/\sqrt{A^2+1} \cdot \ell n |\xi_0| \tag{21}$$

$$\hat{U}_2 = -k^2/2 \cdot [AJ_1 + e_1 \ell n(R_1 - Ae_1 - B) + e_2 \ell n(R_2 + Ae_2 - B) - e_1 - e_2] \tag{22}$$

$$\hat{U}_3 = k^3/6 \cdot [(A^2+2)J_2 + 2ABJ_1 + B^2 I_F] \tag{23}$$

where

$$R_1 = \sqrt{(A^2+1)e_1^2 + 2ABe_1 + B^2}$$

$$R_2 = \sqrt{(A^2+1)e_2^2 - 2ABe_2 + B^2} \tag{24}$$

$$\tilde{I}_F = 1/\sqrt{A^2+1}\cdot[\ell n\,|(A^2+1)e_1 + AB + \sqrt{A^2+1}\cdot R_1\,| + \ell n\,|(A^2+1)e_2 - AB + \sqrt{A^2+1}\cdot R_2\,| - 2\ell n c(y)] \quad (25)$$

$$I_F = \tilde{I}_F - 2/\sqrt{A^2+1}\cdot \ell n\,|\xi_0| \quad (26)$$

$$J_1 = 1/(A^2+1)\cdot[R_1 - R_2 - ABI_F] \quad (27)$$

$$J_2 = 1/2(A^2+1)^2\cdot\{[(A^2+1)e_1 - 3AB]R_1 + [(A^2+1)e_2 + 3AB]R_2 + B^2(2A^2-1)I_F\} \quad (28)$$

The y_0 integrations of the series U_m in Eqs. (18) and (19) are performed analytically with a parabolic approximation for the integrand.

As Eq. (21) has a chordwise logarithmic singularity, it is possible to write $\hat{B}_I = \tilde{B}_I + 2k/\sqrt{A^2+1}\cdot\ell n\,|\xi_0|$. Thus, Eq. (17) can be written as

$$I_1 = \hat{B}_R + i\tilde{B}_I + 2ik/\sqrt{A^2+1}\cdot\ell n\,|\xi_0| \quad (29)$$

B. I_2: The term I_2 can be evaluated approximately by expanding the integrand in powers of y_0, retaining terms up to $\mathcal{O}(y_0)$, and carrying out the y_0 integration, which yields

$$I_2 = \hat{C}_R + i\hat{C}_I \quad (30)$$

$$\hat{C}_R = kA\widehat{U}_{1y_0} - k^2A^2/2\cdot\widehat{U}_{0y_0^2} + \pi k^3A/4\cdot(e_1^2 - e_2^2)/2 \quad (31)$$

$$\hat{C}_I = -kA\widehat{U}_{0y_0} + kA\widehat{U}_{2y0} + k^3A^3/6\cdot\widehat{U}_{0y_0^3} - k^2A^2/2\cdot\widehat{U}_{1y_0^2} + k^3A/2\cdot(e_1^2 - e_2^2)/2 \quad (32)$$

where

$$\widehat{U}_{0y_0} = \ell n(e_1/e_2) + A\tilde{I}_F + \ell n\,|B - R_1 + Ae_1\,| - \ell n[(\sqrt{A^2+1}+A)e_1] - \ell n(\sqrt{A^2+1}\cdot e_2 - B + R_2) + \ell n(\sqrt{A^2+1}\cdot e_2 + B + R_2) - 2A/\sqrt{A^2+1}\cdot\ell n\,|\xi_0| \quad (33)$$

$$\widehat{U}_{1y_0} = -kJ_1 \quad (34)$$

$$\widehat{U}_{0y_0^2} = e_1 + e_2 + AJ_1 + BI_F \quad (35)$$

$$\widehat{U}_{2y_0} = -k^2/2\cdot[AJ_2 + BJ_1/2 + e_1^2/2\cdot\ell n(R_1 - Ae_1 - B) - e_2^2/2\cdot\ell n(R_2 + Ae_2 - B) - (e_1^2 - e_2^2)/4] \quad (36)$$

$$\widehat{U}_{1y_0^2} = -KJ_2 \quad (37)$$

$$\widehat{U}_{0y_0^3} = (e_1^2 - e_2^2)/2 + AJ_2 + BJ_1 \quad (38)$$

Since Eq. (33) has a chordwise logarithmic singularity, one can write $\hat{C}_I = \tilde{C}_I + 2kA^2/\sqrt{A^2+1}\cdot\ell n\,|\xi_0|$. Thus, Eq. (30) becomes

$$I_2 = \hat{C}_R + i\tilde{C}_I + 2ikA^2/\sqrt{A^2+1}\cdot\ell n\,|\xi_0| \quad (39)$$

C. $I_1 + I_2$: Substituting Eqs. (29) and (39) into Eq. (14),

$$I = \hat{B}_R + \hat{C}_R + i(\tilde{B}_I + \tilde{C}_I) + 2ik\sqrt{A^2+1}\cdot\ell n\,|\xi_0| \quad (40)$$

Using this expression, the term SS becomes

$$[SS] = 1/8\pi\cdot[I_R + 2ik\sqrt{A^2+1}\cdot e^{-ikc(y_j)\xi}I_{\ell n}] \quad (41)$$

$$I_R = \int_{-1}^{1} e^{-ikB}(\hat{B}_R + \hat{C}_R + i\tilde{B}_I + i\tilde{C}_I)\bar{C}_p(\xi_1, y_j)c(y_j)\,d\xi_1 \quad (42)$$

$$I_{\ell n} = \int_{-1}^{1} e^{ikc(y_j)\xi_1}\ell n\,|\xi_0|\,\bar{C}_p(\xi_1, y_j)c(y_j)\,d\xi_1 \quad (43)$$

Since $I_{\ell n}$ is the same form as the term appearing in Ref. 2, it can be discretized accurately in the same manner. The result is

$$I_{\ell n} = \frac{2\pi}{2NC+1}\cdot\sum_{k=1}^{NC}\frac{K_{\ell n}e^{ikc(y_j)\xi_k}}{1+\cos\theta_k}\cdot\bar{C}_{pkj}c(y_j)\sin\theta_k \quad (44)$$

$$K_{\ell n} = \sum_{r=0}^{NC-1}[\cos r\theta_k + \cos(r+1)\theta_k]F_r(\theta_i) \quad (45)$$

$$F_r(\theta_i) = -(\ell n 2 + \cos\theta_i) \quad (r=0)$$
$$= -[\cos r\theta_i/r + \cos(r+1)\theta_i/(r+1)] \quad (r \geqq 1) \quad (46)$$

The remaining term I_R can be reduced to a finite sum through the Stark[6] formula because the integrand has a Cauchy singularity and other regular terms. Thus,

$$I_R = \frac{2\pi}{2NC+1}\cdot\sum_{k=1}^{NC}K_R\bar{C}_{pkj}c(y_j)\sin\theta_k \quad (47)$$

$$K_R = e^{-ikB}(\hat{B}_R + \hat{C}_R + i\tilde{B}_I + i\tilde{C}_I) \quad (48)$$

Substituting Eqs. (44) and (47) into Eq. (41),

$$[SS] = \frac{1}{4(2NC+1)}\cdot\sum_{k=1}^{NC}K_k^i\bar{C}_{pkj}c(y_j)\sin\theta_k \quad (49)$$

$$K_k^i = K_R + 2ik\sqrt{A^2+1}\cdot e^{-ikB}/(1+\cos\theta_k)\cdot K_{\ell n} \quad (50)$$

Regular Strip Plus Singular Strip

Combining Eqs. (9) and (49), the downwash contribution from the right wing panel is

$$\left(\frac{\bar{w}_R}{U}\right)_{ij} = \frac{1}{4(2NC+1)}\cdot\sum_{l=1}^{NS}\sum_{k=1}^{NC}[(1-\delta_{l_j})D_{kl}^{ij} + \delta_{lj}K_k^i]\bar{C}_{pkl}c(y_l)\sin\theta_k \quad (51)$$

where δ_{l_j} is the Kronecker delta.

Downwash Contribution from the Left Wing Panel

The downwash contribution from the left wing panel is given by the last term of Eq. (5). On the left wing panel,

$$x_0 = \bar{A}y_0 + \bar{B}$$
$$\bar{A} = -(m_M + \Delta m\xi_1)$$
$$\bar{B} = [2m_M + \Delta m(\xi + \xi_1)]y + c_0(\xi - \xi_1) \quad (52)$$

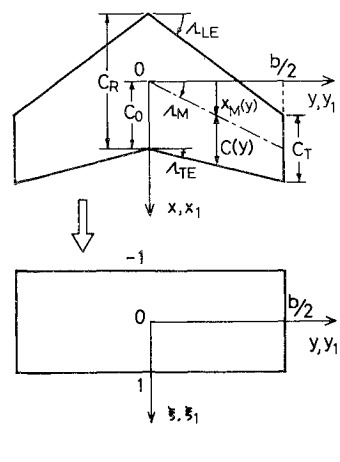

Fig. 1 Geometry and coordinate system.

Since only the control points on the right wing panel are used, all of the strips on the left wing panel have no singularity. Accordingly, the last term of Eq. (5) can be discretized in the same manner as a regular strip. The result is

$$\left(\frac{\bar{w}_L}{U}\right)_{ij} = \frac{1}{4(2NC+1)} \cdot \sum_{l=1}^{NS} \sum_{k=1}^{NC} \bar{D}^{i\,i}_{kl} \bar{C}_{pkl} c(\bar{y}_l) \sin\theta_k \tag{53}$$

$$\bar{D}^{i\,i}_{kl} = \int_{d_l}^{d_{l+1}} \boldsymbol{K}(x_0, \bar{y}_0; k)\, \mathrm{d}\bar{y}_1 \tag{54}$$

$$d_{\bar{l}} = -d_l, \qquad d_{\bar{l}+1} = -d_{l+1} \tag{55}$$

Formulation for the Entire Swept Wing

Combining Eqs. (51) and (53), the downwash equation for the entire swept wing is

$$\left(\frac{\bar{w}}{U}\right)_{ij} = \frac{1}{4(2NC+1)} \cdot \sum_{l=1}^{NS} \sum_{k=1}^{NC} [(1-\delta_{l_j}) D^{i\,j}_{kl} + \delta_{ij} K^i_k + \bar{D}^{i\,j}_{kl}]\, \bar{C}_{pkl} c(y_l) \sin\theta_k \tag{56}$$

where $\bar{C}_{pk\bar{l}} = \bar{C}_{pkl}$ and $c(\bar{y}_{\bar{l}}) = c(y_l)$ are used because the wing is symmetrical.

Numerical Results

The solution of Eq. (56) yields the pressure distribution on the right wing panel. The sectional lift coefficient and the total lift coefficient are given as

$$\bar{C}_l(y_l) = \frac{\pi}{2NC+1} \cdot \sum_{k=1}^{NC} \bar{C}_{pkl} \sin\theta_k \tag{57}$$

$$\bar{C}_L = \frac{(1-s)}{c_0(1+\lambda)} \cdot \frac{2\pi}{NS(2NC+1)} \cdot \sum_{l=1}^{NS} c(y_l) \sum_{k=1}^{NC} \bar{C}_{pkl} \sin\theta_k \tag{58}$$

Figure 2 shows the pressure distribution for a wing with a 45-deg leading-edge sweep, an aspect ratio of 2, a taper ratio of 0.5, a reduced frequency of 1.0, and downwash $\bar{w}/U = -1.0$. In this figure, the number of loading points is 6×10 and the dots on the pressure curves represent the solution of Eq. (56).

Figure 3 compares the spanload distribution between the present method and the doublet-lattice method (DLM) of Ref. 1 for the same wing as in Fig. 1. With as few as 4×5 loading points, the distribution from the present method compares very well with that from the DLM using 10×40 loading points.

Figures 4 and 5 show $\bar{C}_L$ convergence of the present method. It is to be noted that the method greatly improves the

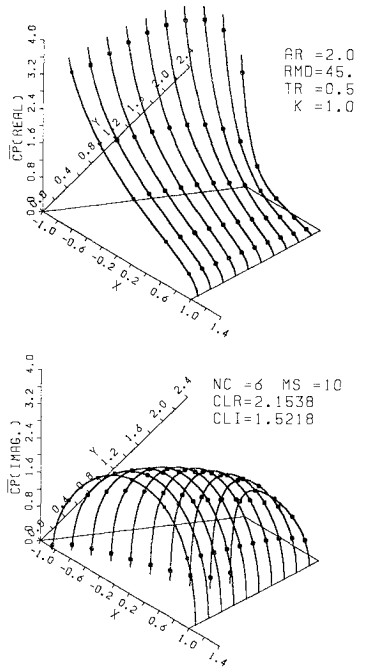

Fig. 2 Example of pressure distribution on swept tapered wing ($\Lambda_{LE} = 45$ deg, $\mathcal{R} = 2$, $\lambda = 0.5$, $k = 1.0$, $\bar{w}/U = -1.0$, $NC = 6$, $NS = 10$).

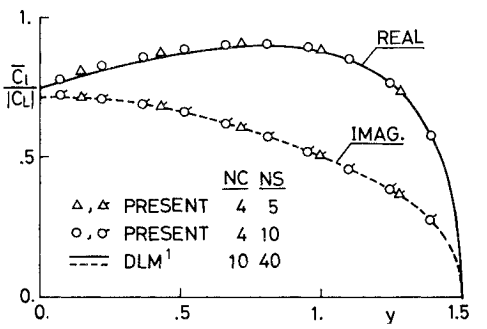

Fig. 3 Comparison of spanload distribution between present method and doublet lattice method ($\Lambda_{LE} = 45$ deg, $\mathcal{R} = 2$, $\lambda = 0.5$, $k = 1.0$, $\bar{w}/U = -1.0$).

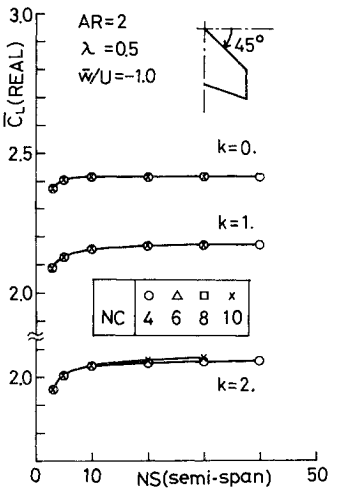

Fig. 4 Effect of the number of loading points on $\bar{C}_L$ (real part).

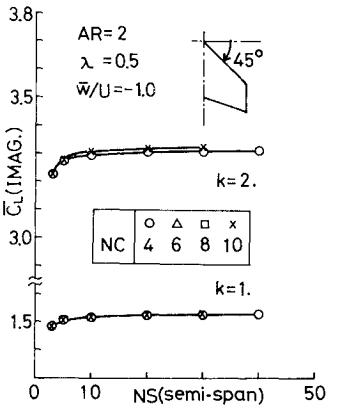

Fig. 5 Effect of the number of loading points on $\bar{C}_L$ (imaginary part).

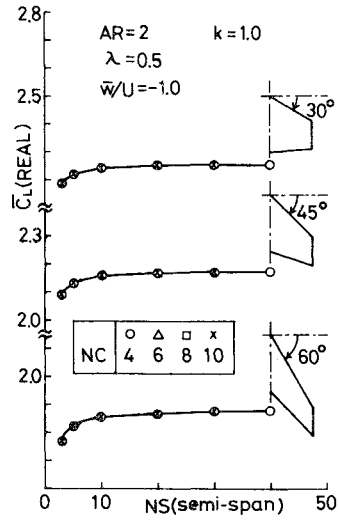

Fig. 6 Effect of leading-edge sweep on $\bar{C}_L$ (real) convergence.

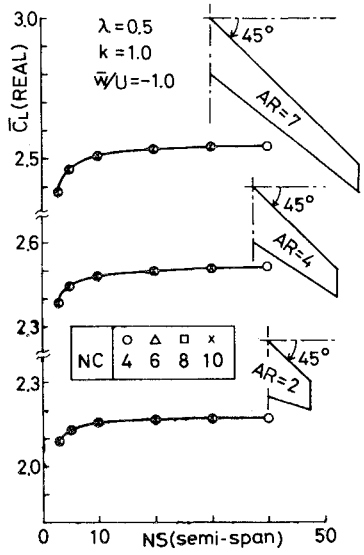

Fig. 7 Effect of aspect ratio on $\bar{C}_L$ (real) convergence.

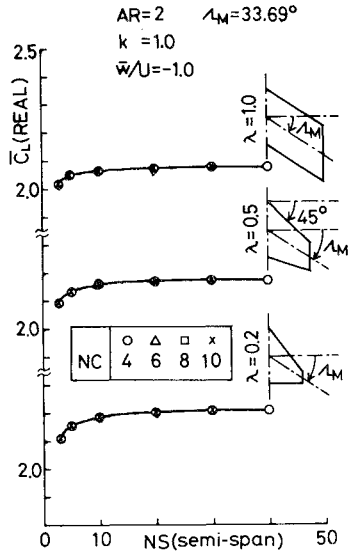

Fig. 8 Effect of taper ratio on $\bar{C}_L$ (real) convergence.

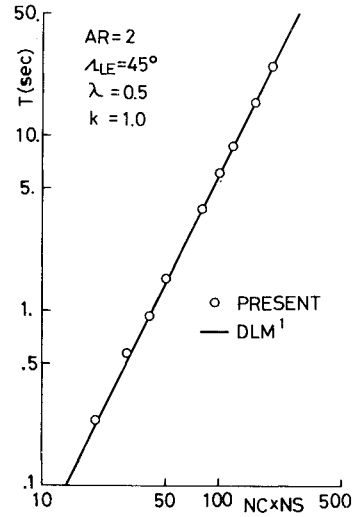

Fig. 9 Comparison of computational time between present method and doublet-lattice method (with FACOM M-382 computer).

convergence for moderate reduced frequency as well as for relatively high reduced frequency.

It can be seen that the method with $NC=4$ and $NS=10$ results in a converged solution at $k=2.0$.

Figures 6-8 show the effect of wing geometry on convergence. Only the real part of $\bar{C}_L$ is given in these figures. It should be noted that the method gives excellent convergence in any case.

Figure 9 compares the computational time between the present method and the DLM. The examples computed herein. were performed on a FACOM-M382 computer in Nagoya University. It can be seen that the computational time for the present method is almost the same as for the DLM with the same number of unknowns.

Conclusions

An improved numerical method (doublet strip method) for calculating the lift distributions on unsteady tapered wings in incompressible flow has been developed. For convenience in the analysis, the swept tapered wing is transformed into a rectangular domain. In the strip containing the control point, the kernel function is treated in expansion series form and many singularities are properly accounted for.

The present method shows excellent convergence of solution for moderate reduced frequency as well as for relatively high reduced frequency. The computational time for the method is almost the same as for the doublet-lattice method with the same number of unknowns.

References

[1]Albano, E. and Rodden, W. P., "A Doublet Lattice Method for Calculating Lift Distributions on Oscillating Surface in Subsonic Flow," *AIAA Journal*, Vol. 7, Feb. 1969, pp. 279-285.

[2]Ichikawa, A. and Ando, S., "Improved Numerical Method for Unsteady Lifting Surfaces in Incompressible Flow," *Journal of Aircraft*, Vol. 20, July 1983, pp. 612-616.

[3]Ueda, T., "Expansion Series of Integral Functions Occurring in Unsteady Aerodynamics," *Journal of Aircraft*, Vol. 19, April 1982, pp. 345-347.

[4]Ando, S. and Ichikawa, A., "The Use of an Error Index to Improve Numerical Solutions for Unsteady Lifting Airfoils," *AIAA Journal*, Vol. 21, Jan. 1983, pp. 47-54.

[5]Hough, G. R., "Remarks on Vortex-Lattice Methods," *Journal of Aircraft*, Vol. 10, May 1973, pp. 314-317.

[6]Stark, V. J. E., "A Generalized Quadrature Formula for Cauchy Integrals," *AIAA Journal*, Vol. 9, Sept. 1971, pp. 1854-1855.